Marchetti, B., Karsili, T. N. V., & Ashfold, M. N. R. (2019). Exploring Norrish type I and type II reactions: an ab initio mechanistic study highlighting singlet-state mediated chemistry. *Physical Chemistry Chemical Physics*, *21*(26), 14418-14428. https://doi.org/10.1039/C8CP07292B, https://doi.org/10.5523/bris.1shnooapazkr528t0hgrffg82v

Exploring Norrish Type I and Type II Reactions: An *ab initio* Mechanistic Study Highlighting Singlet-State Mediated Chemistry.

Barbara Marchetti[†], Tolga N. V. Karsili[†,*] and Michael N. R. Ashfold[‡]

[†]*Department of Chemistry, University of Louisiana at Lafayette, Lafayette, LA 70503, USA*

[‡]*School of Chemistry, University of Bristol, Bristol, BS8 1TS, UK*

*author to whom correspondence be addressed:

Email: tolga.karsili@lousiana.edu

Abstract

Norrish reactions are important photo-induced reactions in mainstream organic chemistry and are implicated in many industrially and biologically relevant processes and in the processing of carbonyl molecules in the atmosphere. The present study reports multi-reference electronic structure calculations designed to assess details of the potential energy profiles associated with the Norrish type-I and type-II reactions of a prototypical ketone 5-methyl-hexan-2-one. We show that the well-established 'triplet state mediated' reaction pathways following initial population of a singlet excited state can be complemented by (hitherto rarely recognized) 'singlet state only' Norrish type-I and type-II reaction mechanisms that involve no spin-forbidden transitions along the respective reaction paths, and suggest how the efficiencies of such reactions might be affected by strategic substitutions at selected sites within the parent ketone.

1. Introduction

Molecular photochemistry has attracted ever growing attention since the mid 19th century.[1] Curious scientists arranged volumetric flasks of solutions in daylight and observed wide ranging color changes – paving the way for light-induced chemistry. Ciamician's seminal work on the 'photochemistry of the future' anticipated the need for the conversion of solar energy into chemical energy as a source of clean and renewable energy.[2] The need to harness sunlight to drive chemical reactions has never been more pressing – as evidenced, for example, by the great current interest in developing photocatalysts for artificial photosynthesis and water-splitting, wherein water is converted into H_2 and O_2.[3,4] Computational and theoretical chemistry has guided improvements in our understanding of the photochemistry of simple molecular systems.[5–11] It is now recognized that many of the key non-radiative transitions in molecular photochemistry occur in regions of configuration space where the potential energy (PE) surfaces of the participating states (*e.g.* the ground and an excited state) become degenerate. When modes orthogonal to the reaction coordinate are considered, these regions of degeneracy develop into conical intersections (CI), which are critical to many of the ultrafast energy-transfer processes in molecular photochemistry.[12,13]

Mechanistic organic photochemistry is filled with elementary reactions that underpin the total synthesis of larger and more versatile molecular structures.[14–18] CIs are intimately involved in many (if not all) of these elementary photoreactions and the non-adiabatic couplings they enable can be imprinted onto the photoreaction dynamics and/or the stereochemistry of the products.[8,19–23] Observations of such electronic and geometric propensities have inspired the development of rules for predicting the outcomes of classes of photoreactions. The Woodward-Hoffmann rules, for example, show how the course of a given reaction (*e.g.* a cycloaddition, electrocyclization,

sigmatropic shift reaction, *etc*.) can be understood in terms of the symmetries and occupancies of π and $\pi*$ orbitals.[24,25] The rules enable prediction as to whether a given reaction will be allowed or forbidden and, of relevance in the present context, whether a thermally disallowed reaction on the ground state PE surface might be allowed photochemically – since the reaction now proceeds on an excited state PE surface. The electrocyclization reaction of 1,3,5-hexatriene is a classic example: the thermally driven electrocyclization of the terminal C-atoms involves rotation and alignment of the π-orbitals in a disrotatory manner, whilst the electrocyclization following photoexcitation is conrotatory.

There are many other families of light-driven reactions. Well-known examples include reactions of conjugated cyclic systems to yield new cyclic compounds with a different number of ring atoms (*e.g*. bicyclic systems or fulvenic structures),[26] photoinduced bond fissions (photodissociations) [27–30] and intra- and intermolecular proton transfer (PT) reactions.[31–34] The latter reaction types form the foundations of Norrish type I and type II reactions[35] (the focus of this manuscript) and have attracted much recent attention.[36–40] The photodissociation of heteroaromatic (*e.g*. indole and pyrrole) and heteroatom containing (*e.g*. (thio)phenol and aniline) molecules are known to proceed (directly or indirectly) *via* $\pi\sigma*$ states, in which the $\sigma*$ orbital is localized around the Y–X bond (where Y is the heteroatom and X is a leaving group (typically X = H and CH_3)).[29,41] PT reactions, on the other hand, proceed *via* charge-transfer (CT) states that lead to an intra- or inter-molecular charge-imbalance which can be neutralized by PT.

Norrish type I and II reactions involve photoexcitation of a carbonyl compound. In the former, the C–C bond adjacent to the carbonyl (*i.e*. a bond to the α carbon) cleaves. Depending on the environment, this may be followed by rearrangement on the ground state PE surface to form a

pair of stable products. Norrish type II reactions (sometimes termed Yang reactions[42]), in contrast, involve an intramolecular H-atom transfer from a more distant carbon (*e.g.* a γ-carbon) to the carbonyl oxygen, followed by eventual C–C bond cleavage – yielding a pair of stable ground state molecules – or rearrangement (cyclization). The latter finds use in synthetic chemistry (*e.g.* the Paternò-Büchi reaction[43]), while Norrish type I and II reactions have been implicated in the photochemical processing of gas phase carbonyl molecules and secondary organic aerosol in the Earth's atmosphere.[44] Norrish type I and II reactions are traditionally described in terms of an initial spin-allowed electronic excitation to a singlet excited state, which is then proposed to undergo intersystem crossing (ISC) to a near-lying triplet state, followed by eventual reaction. Many prior studies have explored the participation of triplet states in the photoinduced reactivity of carbonyl species. The triplet state may show enhanced reactivity (*cf.* the ground S_0 state) and may act as a doorway state for further non-radiative decay to high S_0 state levels. The interplay between singlet and triplet states is thus important to understanding eventual product formation following photoexcitation of ketone and aldehydes.

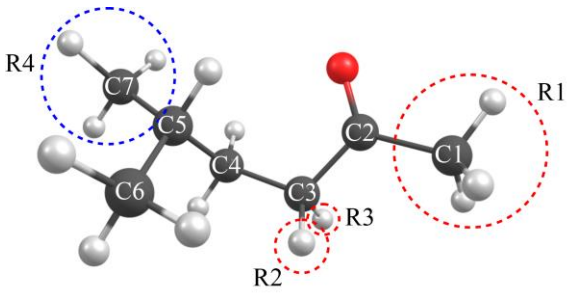

Figure 1: Minimum energy geometry of 5-MHONE. Carbon atoms 1-5 are specifically reference in the text and the labels R1-R4 indicate the groups at which substitution will be investigated.

The present study employs high-level multi-reference electronic structure methods to examine the PE profiles associated with the Norrish type I and type II reactions of one carefully selected ketone – 5-methyl-hexan-2-one (henceforth 5-MHONE; shown in fig. 1) – and investigates the extent to which such reactions might occur without spin-flipping, *i.e*. *via* singlet states only. 5-MHONE is a logical prototype for investigating both Norrish type I and II photoreactions in a self-consistent manner, and the calculated outputs are used to guide our understanding of the likely outcomes of such reactions under isolated molecule conditions (*i.e*. in the absence of any stabilizing collisions) and in the presence of (weakly interacting) solvent molecules that will encourage caging, geminate recombination, and eventual relaxation into the various minima on the S_0 PES.

C2–C3 (or α) bond cleavage in the Norrish type I reaction under collision-free conditions yields radical species whose stability will depend on the degree of substitution and the nature of the substituent(s) near the radical sites (specifically at the sites labelled as R1, R2 and R3 in fig. 1). The present study identifies a CI *en route* to dissociation, at long C2–C3 bond lengths, which offers a possible non-radiative 'all singlet state' route to the S_0 state and alternative rearrangement products, which can be expected to become increasingly important in collisional environments – especially in appropriately substituted carbonyls. The γ-hydrogen (on carbon 5; C5) in 5-MHONE is mandatory for a Norrish type II reaction and enables proton transfer to the carbonyl group. Attaching two methyl groups to C5 in 5-MHONE ensures that one of the radical sites in the biradical intermediate in the Norrish type II reaction involves a tertiary carbon atom, and is thus (relatively) stabilized. Again, we investigate the effects of substitution – specifically how replacing one of the methyl groups on C5 (site R4 in figure 1) with an electron donating (withdrawing) substituent lowers (raises) the energy of the conical intersection identified in the

PT coordinate and thus the likely importance (or otherwise) of the 'all singlet state' Norrish type II route to the S_0 PE surface and eventual stable ground state products.

2. Computational methods

The minimum energy geometry of the ground (S_0) state of 5-MHONE was optimized at complete active space self-consistent field (CASSCF) method and Møller-Plesset second-order perturbation theory (MP2)[45] with a Pople basis set of 6-31G(*d*)[46]. In the CASSCF computations, an active space of eight electrons in seven orbitals (comprising of the four highest occupied and three lowest unoccupied orbitals) was used (henceforth referred to as 8/7). The associated reaction products were optimized at the MP2/6-31G(*d*) level of theory. Transition states (TSs) connecting the optimized minima were computed at the same level of theory using the Berny optimization method.[47] The validity of the TSs were confirmed by conducting intrinsic reaction path computations, which shows that the minimum energy reverse and forward reactions lead to the parent molecule and the appropriate product, respectively.

CIs, between the ground and first excited singlet states of 5-MHONE were optimized using the complete active space self-consistent field (CASSCF) method. As for the ground state, these computations used a state-averaged reference wavefunction, the same 8/7 active space and the 6-31G(*d*) Pople basis set.

Potential energy (PE) profiles connecting the ground state minimum energy geometries to the various CIs were computed using the complete active space second-order perturbation theory (CASPT2)[48–50] method, based on a state-averaged CASSCF reference wavefunction including four singlet states and three triplet states (SA7-CASSCF) coupled with a Dunning's basis set of augmented valence double ζ quality (AVDZ). The same 8/7 active space as described above was

used. The occupied orbitals comprised the p_x and p_y orbitals on the oxygen atom, the π orbital associated with the carbonyl group and σ orbitals. The virtual orbitals are the π* orbital localized on the carbonyl group, the 3s Rydberg orbital of the oxygen atom and 3p/σ* around the C-C(O) bond that is destined to break in the Norrish type I reaction. An imaginary level shift of 0.5 E_H was used to aid convergence and to mitigate the involvement of intruder states.

All optimizations (minima, TSs and CIs) were performed using Gaussian 09,[51] whilst the CASPT2 computations were performed using Molpro 2010.[52]

The effects of substitution were investigated using the MP2/6-31G(*d*) level of theory for optimization of ground state critical structures (ground state reactant and products and the intervening TS). As for 5-MHONE, CASSCF(8,7)/6-31G(*d*) was employed for optimization of CI between the ground and first excited states: the energy of the CI was then calculated at the CASPT2(8,7)/AVDZ level of theory. The CASSCF(8,7)/CASPT2(8,7) calculations for the CN-substituted ketones included three singlet and two triplet states whilst all other substituted carbonyls reported here employed the same state averaging as for 5-MHONE.

3. Results and discussion

3.1 Ground state structures and vertical excitation energies for 5-MHONE

Cartesian coordinates describing the minimum energy and transition state structures optimized in the present work are listed as supporting information (SI). The ground state minimum energy geometry of 5-MHONE is displayed in fig. 1. As expected, the molecule is planar about the sp^2-hybridised carbonyl carbon atom. The other carbon-atoms are sp^3-hybridised and all show local tetrahedral coordination.

Table 1: CASSCF(8,7)/CASPT2(8,7)/AVDZ vertical excitation energies and associated oscillator strengths for transitions to the first three singlet and triplet excited states of 5-MHONE.

Excited electronic state	Vertical excitation energy / eV	Oscillator strength from S_0 state (*f*)
S_1/ $n\pi^*$	3.90	0.0000
S_2/ *ns*	6.03	0.0202
S_3/ *np*	6.85	0.0078
T_1/ $n\pi^*$	3.55	-
T_2/ $\pi\pi^*$	5.44	-
T_3/ *ns*	5.98	-

Table 1 lists the calculated vertical excitation energies to the first three singlet and triplet excited states of 5-MHONE, along with the oscillator strengths of the singlet excitations. Fig. 2 shows the orbitals (plan and cross-sectional views) and dominant orbital promotions associated with excitation to these singlet excited states. All are localized in the immediate vicinity of the carbonyl moiety. As in other ketones, the S_1 state arises from an $\pi^* \leftarrow n$ transition and has very low oscillator strength while, as in acetone, the S_2 and S_3 states both involve excitation from the *n* orbital to σ^* orbitals with, respectively, substantial 3s and 3p Rydberg character.[53,54] Despite the weak oscillator strength associated with the S_1-S_0, experiments show that the S_1 state is a bright state, responsible for the long wavelength UV absorption. This can be understood by considering that vibronic coupling to the higher lying bright states enhances the absorption cross section to S_1. Such effects are not captured by the present computations since they make use of a

time-independent quantum chemical methods and the states are reasonably well separated at the FC region and there is thus insufficient mixing of electronic configurations in the adiabatic wavefunction. As in acetone,[53] the S_2-S_0 transition is calculated to have the larger oscillator strength.

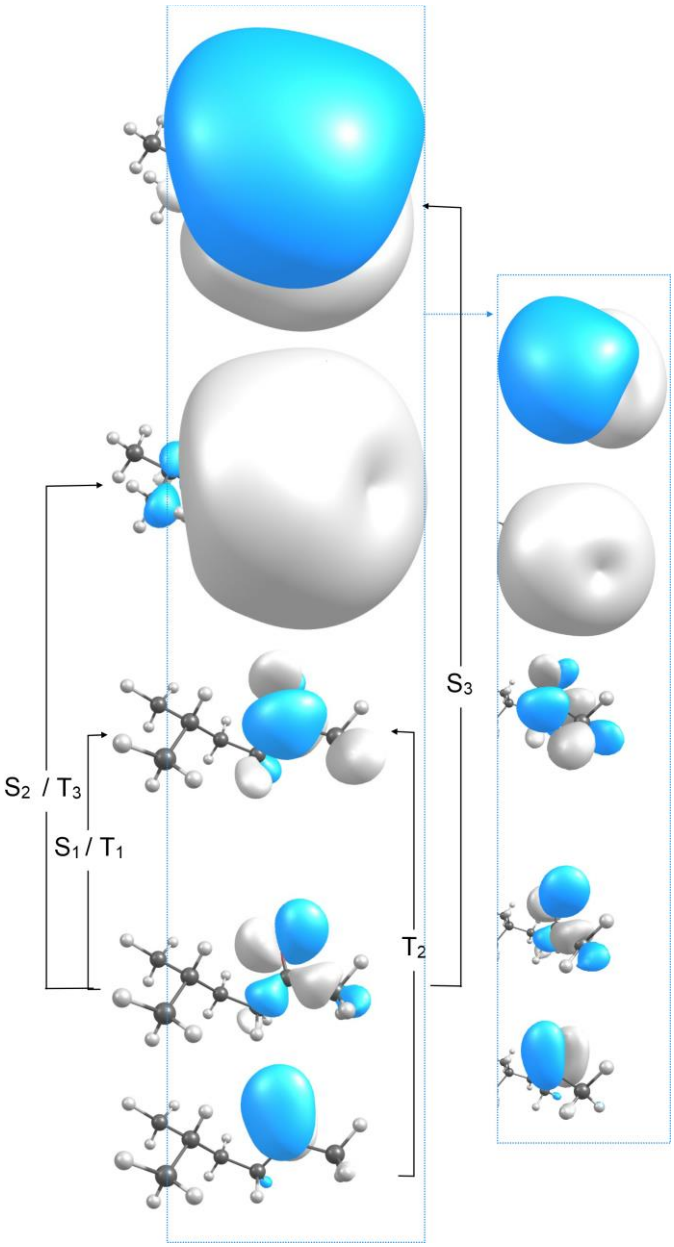

Figure 2: Plan (left) and cross-sectional (to the right) representations of selected orbitals within the active space of the SA-CASSCF(8,7)/CASPT2(8,7) calculations used to compute the first three singlet and triplet vertical transitions of 5-MHONE. The arrows indicate the dominant orbital promotions associated with the computed transitions, *i.e.* $S_1/n\pi^*$, S_2/ns, S_3/np, $T_1/n\pi^*$, $T_2/\pi\pi^*$ and T_3/ns.

As in acetone,[55] the $^1\pi\pi^*$ state is not amongst the first three singlet excited states of 5-MHONE, whereas the corresponding $^3\pi\pi^*$ state is the second excited triplet state. Such an effect is also consistent with the energetic positions of the $^1\pi\pi^*$ and $^3\pi\pi^*$ states of ethene.[56]

3.2 Photoinduced reaction paths for 5-MHONE

Norrish type I reactions.

This reaction involves initial extension of one of the C–C bonds adjacent to the C=O group (*i.e.* α-cleavage). Complete bond rupture is the most likely outcome under collision-free conditions but caging effects and/or geminate recombination reactions in solution will encourage alternative rearrangements to yield stable products. Figure 3 shows a Norrish type I reaction scheme for 5-MHONE. We recognize that photoexcitation could promote C1–C2 or C2–C3 bond extension but, for simplicity, henceforth focus on the latter extension towards $(CH_3)_2CHCH_2CH_2$ + CH_3CO radical products and possible rearrangement to stable product pairs including: (1) CO + $CH_3CH_2CH_2CH(CH_3)_2$, (2) $CH_3CH_2CH(CH_3)_2$ + CH_2CO and (3) CH_2=$CHCH(CH_3)_2$ + CH_3CHO. Our choice to focus on C2-C3 is driven by the diverse range of rearrangement products that are available following C2-C3 bond fission. Nadasdi *et al.* show that the rival dissociation channels in methylethylketone ($CH_3COC_2H_5$) to yield C_2H_5 + CH_3CO *vs.* CH_3 + C_2H_5CO display very similar energetics [57] and such similarities can be expected to extend to 5-

MHONE also. We do recognize however that photoinduced C1-C2 fission, which leads to the formation of CH_3 + CO $CH_2CH_2CH(CH_3)_2$ products, may compete with C2-C3 bond fission. By analogy with acetaldehyde,[58] we might expect the nascent products to fail to fully separate and re-encounter to give CH_4 + $COCHCH_2CH(CH_3)_2$ *via* a roaming mechanism.

Figure 4(a) displays the PE profiles associated with the C2–C3 bond coordinate of current interest (henceforth $R_{C–C}$). The ground state (black curve) shows a progressive increase in PE along $R_{C–C}$, but the PE profile for the S_1 state first rises (until $R_{C–C}$ ~1.9 Å), then declines at larger R_{C-C}. This can be understood by recognizing that the excited state configuration (which is predominantly $n\pi^*$ in the vertical region) progressively gains $n\sigma^*$ character upon extending R_{C-C} as shown in the SI (fig. S1). The rise in the S_0 PE profile and the net fall in the PE profile for the S_1 state leads to a crossing (or at least a merger) at $R_{C–C}$ ~ 2.88 Å, which satisfies the requirements of a minimum energy S_1/S_0 CI (henceforth CI_{C-C}) *via* optimization of a degeneracy between the ground and excited states with infinite derivative coupling. $R_{C–C}$ in fig. 4a is derived as an (unrelaxed) linear interpolation in internal coordinates (LIIC) linking the geometries of the S_0 minimum and CI_{C-C}. Despite the near asymptotic geometry of CI_{C-C}, internal conversion is expected to yield a highly vibrational excited S_0 molecule, with energies well in excess of transition states TS 1, 2 and 3. As such excitation at energies greater than or equal to the CI_{C-C} energy is likely to encourage distortion along R_{C-C} and dissociation, at a rate that out-competes the rate of any possible intramolecular vibrational energy redistribution R_{C-C}, lead to direct dissociation and outcompete intermolecular vibrational energy redistribution.

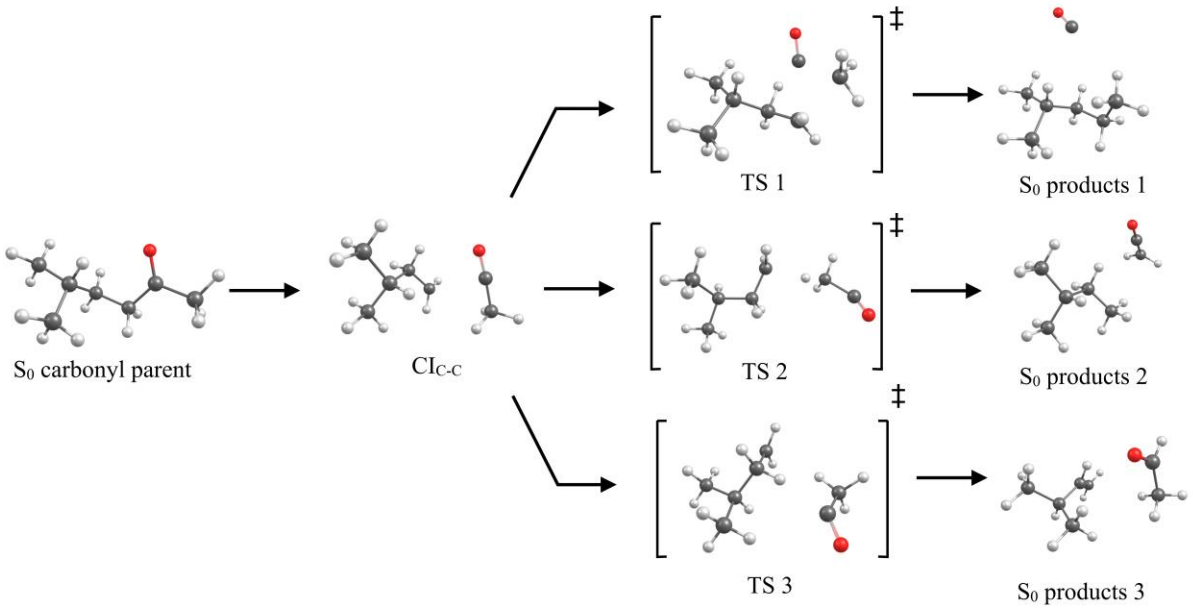

Figure 3: Reaction path associated with the Norrish type I reaction in 5-MHONE

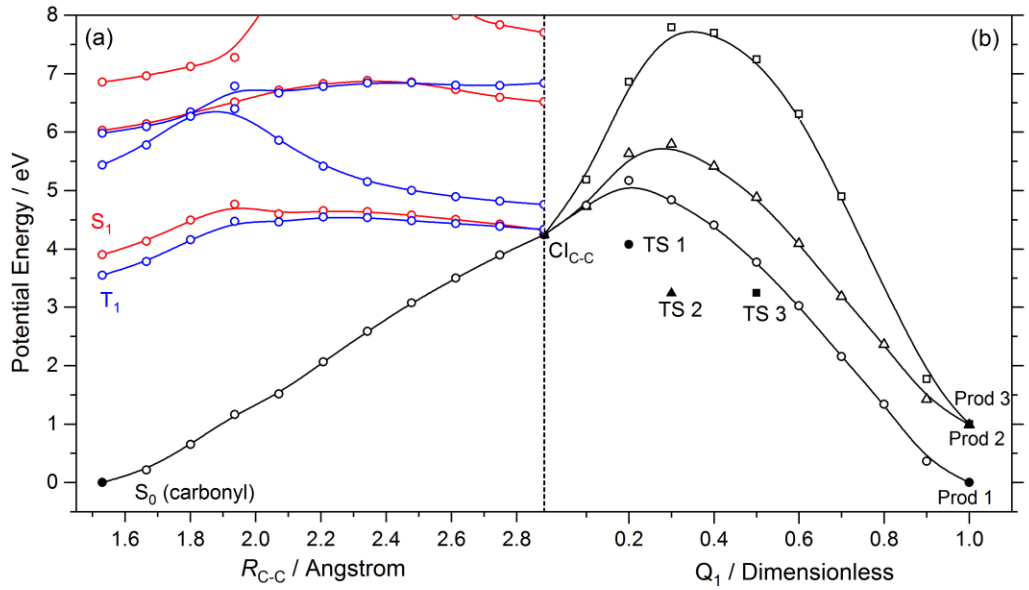

Figure 4: (a) Profiles for the ground (black) and first few singlet (red) and triplet (blue) excited state potentials along the LIIC linking the parent S_0 geometry with $CI_{C–C}$. (b) PE profiles along Q_1, the respective LIICs connecting $CI_{C–C}$ to products 1 (open circles), 2 (open squares) and 3 (open triangles) on the S_0 PES. Filled points represent the energies of the reactant, the transition states (TSs) and the final products on the S_0 PES.

The embryonic fragments at $CI_{C–C}$ are both planar around their respective radical sites (*i.e.* about the carbon atom bearing the odd electron), reflecting the change in hybridization that accompanies C–C bond extension. This enables better alignment of the singly occupied orbital with one of the vicinal C–H bonds, encouraging stabilization by hyperconjugation. The π electrons associated with the carbonyl group in the CH_3CO moiety can provide further stabilization *via* resonance. The optimized $CI_{C\text{-}C}$ structure involves a linear C–C=O backbone and has many parallels with the corresponding CIs identified in recent *ab initio* studies of acetone[59] and methyl ethyl ketone.[57] The bent ground state of the isolated CH_3CO radical[38,60] is the lower component of a Renner-Teller pair with ^2E symmetry at the C_{3v} geometry (with a linear C–C=O spine). Thus $CI_{C–C}$ is best viewed as the approach to an asymptote where, for linear CH_3CO, two singlet (the S_0 and S_1) and two triplet (the T_1 and T_2) PESs of the parent 5-MHONE molecule approach degeneracy. As such, $CI_{C–C}$ can act as a conduit for internal conversion (IC) of S_1 population to high vibrational levels of the S_0 state. This also implies that the ground-state asymptotic energy is necessarily an overestimation to the true dissociation energy, since the minimum energy geometry of the acyl fragment is bent.

The primary focus of this article is to identify possible pure singlet state contributions to Norrish type I (and II) reactions in carbonyls but, for completeness, we note that the calculated vertical excitation energy (VEE) to the T_1 state is ~0.35 eV below that of the S_1 state (Table 1) and that the PE profiles of the T_1 and S_1 states along $R_{C–C}$ (Figure 4) are similar. Thus the region of configuration space associated with $CI_{C–C}$ could also offer enhanced opportunities for ISC, both from the S_1 to T_1 state, and from T_1 to the ground state.

The recognition that the intermediate geometry formed by C–C bond extension constitutes a CI between the S_1 and S_0 PESs of 5-MHONE is important, and complements recent identifications of similar CIs at extended C–C bond lengths in both acetone[59] and methyl ethyl ketone.[38] Non-adiabatic coupling in the vicinity of $CI_{C–C}$ could enable population transfer by IC (from S_1) or ISC (from T_1) into any of several different minima on the S_0 PES. Products (1) – (3) correspond to three of the better documented minima but, as fig. 4(a) shows, IC and/or ISC could also lead to reformation of the starting molecule – a possible outcome that appears not yet to have received much attention in the context of ketone photochemistry. Such a process would commonly be termed photostability, and is a desirable photophysical outcome in many bio-organic molecules.[9,61–63]

Outcomes such as those exemplified by products (1) to (3) in the case of 5-MHONE are well-documented in ketone photochemistry.[42,64] Figure 4(b) shows PE profiles along unrelaxed LIICs (generically labelled Q_1) on the S_0 PES connecting $CI_{C–C}$ to the minima associated with each of products (1) – (3). All three profiles exhibit potential barriers. This is not unexpected, given that an unrelaxed scan necessarily returns an upper limit to the 'true' reaction profile. Optimizing the TSs associated with formation of each of products (1) – (3) on the S_0 PES, starting from the parent S_0 minimum energy geometry, yields lower energy barriers (shown by the filled symbols in fig 4(b)), all of which are below the energy of $CI_{C–C}$. This re-emphasizes the possibility that population accessing the S_0 PES following photoexcitation and non-adiabatic coupling in the vicinity of $CI_{C–C}$ could partition into channels leading to products or to reformation of the original parent molecule. As fig. 4(b) also shows, the formation of Norrish type I products (1) from 5-MHONE is calculated to be the least endoergic process, but this process also shows the highest optimized TS energy on the S_0 PES.

Norrish type II reactions.

The Norrish type II reaction scheme illustrated in fig. 5 involves abstraction of an H atom from a terminal CH_3 group in 5-MHONE by the carbonyl oxygen atom, resulting in an excited state keto-enol tautomerisation. This type of H atom migration is also commonly described as an excited state intramolecular proton transfer (PT) or an excited state intramolecular H atom transfer.[32,65] The biradical intermediate formed by PT is unstable and fragments (reaction 4) yielding the stable products $(CH_3)_2C{=}CH_2$ + $CH_3C(OH){=}CH_2$ or rearranges to form a substituted cyclobutane. The latter reaction (reaction 5) is often termed a Yang cyclization.

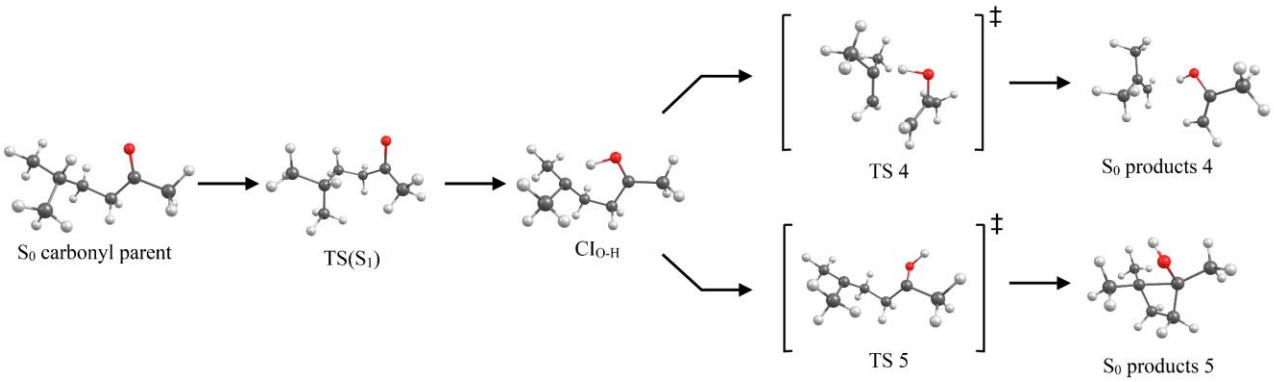

Figure 5: Reaction path associated with the Norrish type II reaction of 5-MHONE

Calculated PE profiles associated with the overall Norrish type II reactions for 5-MHONE are shown in fig. 6. The S_0 (and excited S_1 and T_1) state PE profiles for the initial PT were computed using a LIIC (labelled Q_2 in fig. 6(a)) connecting the minimum energy S_0 geometry (Q_2 = 0) to that of the optimized S_1/S_0 CI (henceforth $CI_{O–H}$) at Q_2 = 1. CI_{O-H} has a geometry (shown in fig. 5) in which an H atom is shared between the tertiary C-atom and the carbonyl O-atom. Its calculated energy is 3.17 eV above the S_0 minimum. The S_1 state reaction path shows an initial rise in PE with increasing Q_2, then declines beyond Q_2 ~0.7. Again, we note that the ~0.5 eV

barrier returned by such a LIIC-based calculation must be an upper limit to the true barrier height and, as fig. 6(a) shows, optimizing the TS (TS(S_1) in fig. 5) connecting the vertical Franck-Condon (FC) and $CI_{O–H}$ geometries yields a value intermediate between the S_1 VEE and the energy of $CI_{O–H}$ – suggesting that the minimum energy reaction path connecting the FC region and $CI_{O–H}$ on the S_1 PES is actually barrierless. We note that the S_1 and S_0 states cross at a slightly smaller Q_2 value than the CI geometry. This small discrepancy arises because the CI was optimized at the CASSCF/6-31G(*d*) level whilst the PE profiles were computed at the CASPT2/cc-pVDZ level.

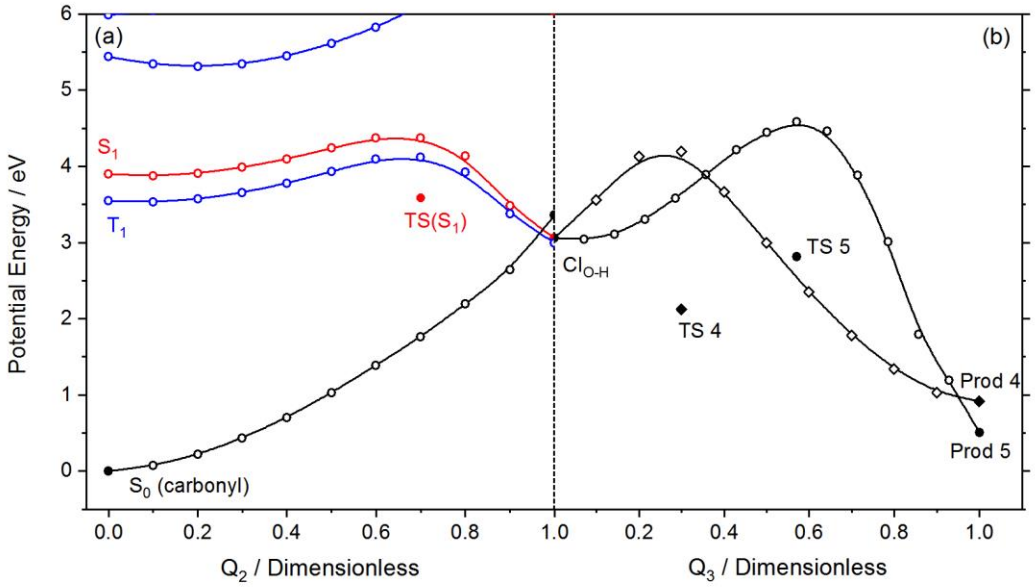

Figure 6: (a) Profiles for the ground (black) and first excited singlet (red) and triplet (blue) state potentials along Q_2, the LIIC linking the parent S_0 geometry with $CI_{O–H}$. (b) PE profiles along Q_3, the respective LIICs connecting $CI_{O–H}$ to products 4 (open diamonds) and 5 (open circles) on the S_0 PES. Filled black points represent the energies of the optimized reactant, transition states (TSs) and final products on the S_0 PES, while the filled red point in (a) shows the optimized energy of TS(S_1) on the S_1 PES.

Beyond $CI_{O–H}$, the intermediate can rearrange via two well-known routes, yielding products labeled 4 and 5 in fig. 5. As fig. 6(b) shows, the PE profiles along the respective LIIC paths (Q_3) connecting $CI_{O–H}$ to these products on the S_0 PES display barriers but, as with the Norrish type I reactions considered previously, the energies of the optimized TSs connecting the S_0 parent molecule to products 4 and 5 are both below that of $CI_{O–H}$ (well below in the case of TS4). Again, reference to fig. 6 suggests that photoexcited 5-MHONE(S_1) molecules that access the S_0 PES by non-adiabatic coupling in the vicinity $CI_{O–H}$ can react on to form products (4) or (5) or reform their starting configuration.

3.3 Substituent effects

Inspection of the reaction mechanisms shown in figs. 3 and 5 suggests that a particular substitution can be expected to affect Norrish type I and II reactions very differently. Norrish type I processes are driven by α-cleavage, so changes to the sites labelled R1, R2 and R3 in fig. 1 are likely to have greater impact than changes to R4. Conversely, Norrish type II reactions involve transfer of a more distant H atom and, in the context of fig. 1, such reactions will more likely be sensitive to changes to R4. Such effects are now considered.

Norrish type I reactions

As shown above, non-adiabatic coupling at configurations around $CI_{C–C}$ can access a range of ground state products. Tables 2 and 3 summarize how selected changes in the substituents at R1, R2 and/or R3 affect the relative stabilities of the ground state reactants and products, the VEEs from the parent S_0 minimum to the S_1 and T_1 states, and the energy of $CI_{C–C}$ (relative to the minimum of the parent S_0 state and to the VEE of the S_1 state).

For orientation, the rows labelled Me, H, H in Tables 2 and 3 represent the parent 5-MHONE. When R1 = H, the parent molecules are aldehydes and reactions 1 and 2 yield the same ground state products. Product channel 3 only operates if the acyl moiety at TS3 contains an H atom. In the context of Tables 2 and 3, we focus on the cases where R1 = Me or *iso*-propyl (*i*-Pr) – in both of which cases the products of reaction 3 are a ketene (along with the corresponding alkane) – but we note the possible reaction 3 when R1 = OH, yielding CO_2 plus an alkane.

Replacing R1 = Me by a bulkier *i*-Pr group has negligible effect on the relative energies of the ground state reactants and products, but is predicted to lead to modest increases in the VEE to the S_1 and T_1 states and in the energy of $CI_{C–C}$. Any mesomeric effects associated with these mainly σ-perturbing alkyl substituents are likely to be similar, so the predicted differences are most likely attributable to differences in steric hindrance.

Substituting R1 or R2/R3 with a single CN group stabilizes products 1, to the extent that their formation from the S_0 state of either CN-substituted parent is predicted to be exoergic. This can be traced to CN-induced destabilization of the parent molecule. CN is a π-accepting substituent, that withdraws electron density from the proximal C=O group. The destabilizing influence of the CN disappears upon forming products 1, however, since the CO is eliminated. Hence the more favorable energetics for reaction 1, *cf*. 5-MHONE.

The destabilization induced by a proximal CN group is also revealed in the VEEs to the S_1 (and T_1) states, both of which are greater than in the reference 5-MHONE parent molecule. The energy of $CI_{C–C}$ is predicted to fall, however. This can be understood by viewing C–C bond extension as the separation of a bonding pair of electrons; one of which can then be stabilized by conjugation with the π*-orbitals of the CN substituent. These contrasting effects on the reactant/product and $CI_{C–C}$ stabilities are repeated (and indeed amplified) in the case that CN is

substituted at both R2 and R3. CN substitution at R1 has little effect on the energetics of reaction 2, whereas the same substitution at R2 substantially reduces the reaction endoergicity. The implicit stabilization of products 2 can be plausibly traced to the destabilization of the parent molecule, in which the π-system is destabilized by a proximal CN-substituent. This destabilization leads to a reduction in the activation barrier for forming products 1 and 2.

As Table 2 and 3 shows, the effects of OH substitution at R1 or R2 show some similarities with those seen with CN, but to a milder extent.

Table 2: Substituent effects on the calculated energies (in eV) of the ground state products of Norrish type I reactions yielding products 1, 2 and 3, each defined relative to that of the corresponding parent ground state minimum.

R1, R2, R3	Products 1 (S_0)	Products 2 (S_0) [#]	Products 3 (S_0) [#]	
H, H, H	-0.09	1.30	--	
Me, H, H	0.21	1.36	1.26	
*i*Pr, H, H	0.24	1.31	1.27	
CN, H, H	-0.25	1.37	--	
H, CN, H	-0.30	0.94	--	
H, OH, H	-0.03	1.19	--	
H, OH, OH	0.02	1.22	--	
H, CN, OH	-0.13	1.09	--	
H, CN, CN	-0.30	0.74	--	

[#] Products 1 and 3 are the same when R1 = H.

Table 3: Substituent effects on the vertical excitation energies (VEEs) of the S_1 and T_1 states and on the energy of $CI_{O–H}$ (defined relative to the S_0 minimum energy and to the S_1 state VEE), in eV.

R1, R2, R3	VEE (T_1–S_0)	VEE (S_1–S_0)	$CI_{C–C}$	ΔE ($CI_{C–C}$ – S_1)
H, H, H	3.62	4.03	3.84	–0.19
Me, H, H	3.55	3.90	4.24	0.34
*i*Pr, H, H	3.75	4.11	4.59	0.48
CN, H, H	4.01	4.12	4.06	–0.06
H, CN, H	3.72	4.09	3.36	–0.73
H, OH, H	3.77	4.17	3.80	–0.37
H, OH, OH	3.69	4.11	3.72	–0.39
H, CN, OH	3.49	4.01	3.56	–0.45
H, CN, CN	3.71	4.09	3.22	–0.87

Norrish type II reactions

Our investigations of Norrish type II reactions are limited to the effects of substituting the Me group at R4 by an H atom, by one strongly π-withdrawing species (CN) and by one classic π-donating group (OMe). Table 4 shows that either of the latter substitutions destabilizes products 4 (*cf.* 5-MHONE). CN substitution renders the neighboring C=C bond electron-deficient, while the π-donating OMe substituent leads to an increase in electron-pair repulsion around the C=C bond – both of which result in a net destabilization. CN and OMe substitution at R4 destabilizes products 5 also (*cf.* 5-MHONE), but this is a much milder effect. Indeed, as Table 4 shows, when compared to the case that R4 = H, CN or OMe substitution might be viewed as offering a modest stabilization of products 5. Both of these effects can be rationalized by recognizing that the Me group provides a +I inductive effect which helps stabilize the (geometrically strained, solely σ-

bonded) cyclobutane product – a benefit that is lost upon replacing the Me group by H or by the π-perturbing substituents.

Despite their very different □-perturbing capabilities, Table 5 shows that replacing the Me group with either a CN or an OMe substituent has minimal effect on the energy of $CI_{O–H}$ (defined relative to the S_0 state minimum).

Table 4: Substituent effects on the calculated energies (in eV) of the ground state products of Norrish type II reactions yielding products 4 and 5, each defined relative to that of the corresponding parent ground state minimum. 5-MHONE corresponds to the case that R4 = Me.

R4	Products 4 (S_0)	Products 5 (S_0)
Me	0.92	0.51
H	1.74	0.89
CN	1.69	0.67
OMe	1.54	0.70

Table 5: Substituent effects on the vertical excitation energies (VEEs) of the S_1 and T_1 states and on the energy of $CI_{C–C}$ (defined relative to the S_0 minimum energy and to the S_1 state VEE), in eV. 5-MHONE corresponds to the case that R4 = Me.

R4	VEE (T_1–S_0)	VEE (S_1–S_0)	$CI_{O–H}$	ΔE ($CI_{O–H}$ – S_1)
Me	3.55	3.90	3.17	–0.73
H	3.52	3.90	3.20	–0.70
CN	3.19	4.18	3.16	–1.02
OMe	3.77	4.15	3.19	–0.96

4. General Discussion and Conclusions

Norrish type I reactions in ketones have traditionally been described in terms of photon absorption to yield an excited singlet state molecule, ISC to a near lying triplet state, followed by cleavage of an α carbon bond. The probability of ISC in these carbonyl compounds is enhanced by the comparatively large spin-orbit couplings in the region of singlet-triplet avoided crossings at geometries near the photoexcited singlet state minimum. Triplet-state mediated dissociation is also a logical interpretation, given that a triplet arrangement of electrons is the simplest way of achieving a long-range repulsive interaction between the separating radical fragments.

More recent studies recognize the possibility of C–C bond fission in either excited state, and the present work explores the PE profiles associated with Norrish type I (and Norrish type II) reactions in a model ketone, 5-MHONE, with the aim of highlighting likely singlet excited state contributions to the observed chemistry. For simplicity, we have focused on just one of the α carbon bonds, and identified a S_1/S_0 CI ($CI_{C–C}$) that is very reminiscent of those identified in recent studies of acetone and methyl ketone.[53,57,59] As in these smaller ketones, the optimized CI_{C-C} structure involves a large R_{C-C} separation and a linear C–C=O backbone in the emergent carbonyl fragment – an orbitally degenerate radical that, upon full separation and bending, would split into a Renner-Teller pair of states. CI_{C-C} provides a route for non-adiabatic coupling from the S_1 state to high vibrational levels of the S_0 state with a total energy in excess of the TSs associated with formation of any or all of rearrangement products 1, 2 or 3 or with reformation of the starting 5-MHONE structure on the S_0 PES. Clearly, the C–C bond fission products can also arise via the 'traditional' ISC driven mechanism, and the ground state rearrangement products 1–3 can arise via successive (*i.e.* $S_1 \rightarrow T_1 \rightarrow S_0$) ISC steps. Thus the most striking finding from the present work is the demonstration that Norrish type I photoreactions can occur via triplet state

mediated *and* purely singlet state mechanisms, and that the relative importance of these rival processes is likely to be molecule, excitation wavelength and phase (solution *vs* gas) dependent. Proton-transfer reactions in general, and Norrish type II reactions in particular, are more widely recognized as proceeding via singlet and triplet mediated mechanisms. The C-atom in 5-MHONE would be considered a poor H-atom donor (*cf.* N–H, O–H, *etc*. bonds where the donor is an acidic site and singlet states are known to prevail in the associated proton transfer). But, just as in these better established cases, we find that the characteristic evolution from a locally excited orbital to charge transfer orbital character persists in the present case of the C-atom donor also.

Acknowledgements

TNVK thanks the University of Louisiana at Lafayette for start-up funds. MNRA is grateful to the Engineering and Physical Sciences Research Council for funding through a Programme Grant (EP/L005913).

Additional outputs that underpin data reported in this paper have been placed in the University of Bristol's research data repository and can be accessed using the following DOI: 10.5523/bris.1shnooapazkr528t0hgrffg82v.

References

1 K. Glusac, What has light ever done for chemistry?, *Nat. Chem.*, 2016, **8**, 734.

2 G. Ciamician, THE PHOTOCHEMISTRY OF THE FUTURE, *Science (80-.).*, 1912, **36**, 385–394.

3 A. FUJISHIMA and K. HONDA, Electrochemical Photolysis of Water at a Semiconductor Electrode, *Nature*, 1972, **238**, 37.

4 S. Chu, W. Li, Y. Yan, T. Hamann, I. Shih, D. Wang and Z. Mi, Roadmap on solar water splitting: current status and future prospects, *Nano Futur.*, 2017, **1**, 22001.

5 O. P. J. Vieuxmaire, Z. Lan, A. L. Sobolewski and W. Domcke, *Ab initio* characterization of the conical intersections involved in the photochemistry of phenol, *J. Chem. Phys.*, 2008, **129**, 224307.

6 J. J. Serrano-Pérez, M. J. Bearpark and M. A. Robb, The extended S1/S0 conical intersection seam for the photochemical 2 + 2 cycloaddition of two ethylene molecules, *Mol. Phys.*, 2012, **110**, 2493–2501.

7 S. Boldissar and M. S. de Vries, How nature covers its bases, *Phys. Chem. Chem. Phys.*, 2018, **20**, 9701–9716.

8 A. L. Sobolewski and W. Domcke, Conical intersections induced by repulsive 1πσ* states in planar organic molecules: malonaldehyde, pyrrole and chlorobenzene as photochemical model systems, *Chem. Phys.*, 2000, **259**, 181–191.

9 R. Improta, F. Santoro and L. Blancafort, Quantum Mechanical Studies on the Photophysics and the Photochemistry of Nucleic Acids and Nucleobases, *Chem. Rev.*, 2016, **116**, 3540–3593.

10 B. Marchetti, T. N. V. Karsili, M. N. R. Ashfold and W. Domcke, A 'bottom up', ab initio computational approach to understanding fundamental photophysical processes in nitrogen containing heterocycles, DNA bases and base pairs, *Phys. Chem. Chem. Phys.*, 2016, **18**, 20007–20027.

11 M. Barbatti, A. C. Borin and S. Ullrich, Photoinduced processes in nucleic acids, *Top. Curr. Chem.*, 2015, 355, 1-32.

12 W. Domcke, D. R. Yarkony and H. Koeppel, *Conical Intersections: Theory, Computation and Experiment*, 2011.

13 W. Domcke, D. R. Yarkony and H. Koeppel, *Conical Intersections: Electronic Structure, Dynamics & Spectroscopy*, 2004.

14 H. D. Roth, The Beginnings of Organic Photochemistry, *Angew. Chemie Int. Ed. English*, 1983, **28**, 1193–1207.

15 R. B. Woodward, F. J. Brutschy and H. Baer, The Structure of Santonic Acid, *J. Am. Chem. Soc.*, 1948, **70**, 4216–4221.

16 N. Hoffmann, Photochemical Reactions as Key Steps in Organic Synthesis, *Chem. Rev.*, 2008, **108**, 1052–1103.

17 J. P. Knowles, L. D. Elliott and K. I. Booker-Milburn, Flow photochemistry: Old light

through new windows, *Beilstein J. Org. Chem*, 2012, **8**, 2025–2052.

18 M. D. Kärkäs, J. A. Porco and C. R. J. Stephenson, Photochemical Approaches to Complex Chemotypes: Applications in Natural Product Synthesis, *Chem. Rev.*, 2016, **116**, 9683–9747.

19 S. Perun, A. L. Sobolewski and W. Domcke, Conical Intersections in Thymine, *J. Phys. Chem. A*, 2006, **110**, 13238–13244.

20 C. Xie, C. L. Malbon, D. R. Yarkony, D. Xie and H. Guo, Signatures of a Conical Intersection in Adiabatic Dissociation on the Ground Electronic State, *J. Am. Chem. Soc.*, 2018, **140**, 1986–1989.

21 W. Credo Chung, Z. Lan, Y. Ohtsuki, N. Shimakura, W. Domcke and Y. Fujimura, Conical intersections involving the dissociative 1pisigma* state in 9H-adenine: a quantum chemical ab initio study., *Phys. Chem. Chem. Phys.*, 2007, **9**, 2075–84.

22 T. J. Martinez, Seaming is believing, *Nature*, 2010, **467**, 412.

23 M. H. Farag, T. L. C. Jansen and J. Knoester, Probing the Interstate Coupling near a Conical Intersection by Optical Spectroscopy, *J. Phys. Chem. Lett.*, 2016, **7**, 3328–3334.

24 R. Hoffmann and R. B. Woodward, Selection Rules for Concerted Cycloaddition Reactions, *J. Am. Chem. Soc.*, 1965, **87**, 2046–2048.

25 R. B. Woodward and R. Hoffmann, The Conservation of Orbital Symmetry, *Angew. Chemie Int. Ed. English*, 2018, **8**, 781–853.

26 Q. Li, D. Mendive-Tapia, M. J. Paterson, A. Migani, M. J. Bearpark, M. A. Robb and L. Blancafort, A global picture of the S1/S0 conical intersection seam of benzene, *Chem. Phys.*, 2010, **377**, 60–65.

27 Z. Lan, W. Domcke, V. Vallet, A. L. Sobolewski and S. Mahapatra, Time-dependent

quantum wave-packet description of the1πσ* photochemistry of phenol, *J. Chem. Phys.*, 2005, 122, 225315.

28 A. L. Devine, M. G. D. Nix, R. N. Dixon and M. N. R. Ashfold, Near-Ultraviolet Photodissociation of Thiophenol, *J. Phys. Chem. A*, 2008, **112**, 9563–9574.

29 M. N. R. Ashfold, B. Cronin, A. L. Devine, R. N. Dixon and M. G. D. Nix, The role of pisigma* excited states in the photodissociation of heteroaromatic molecules., *Science*, 2006, **312**, 1637–40.

30 D. A. Blank, S. W. North and Y. T. Lee, The ultraviolet photodissociation dynamics of pyrrole, *Chem. Phys.*, 1994, **187**, 35–47.

31 X. Wu, T. N. V. Karsili and W. Domcke, Excited-State Deactivation of Adenine by Electron-Driven Proton-Transfer Reactions in Adenine-Water Clusters: A Computational Study, *ChemPhysChem*, 2016, **17**, 1298–1304.

32 A. L. Sobolewski and W. Domcke, Photoinduced electron and proton transfer in phenol and its clusters with water and ammonia, *J. Phys. Chem. A*, 2001, **105**, 9275–9283.

33 R. Szabla, R. W. Góra, M. Janicki and J. Šponer, Photorelaxation of imidazole and adenine via electron-driven proton transfer along H_2O wires, *Faraday Discuss.*, 2016, **195**, 237–251.

34 S. Perun, A. L. Sobolewski and W. Domcke, Role of electron-driven proton-transfer processes in the excited-state deactivation of the adenine-thymine base pair, *J. Phys. Chem. A*, 2006, **110**, 9031–9038.

35 R. G. W. NORRISH and C. H. BAMFORD, Photo-decomposition of Aldehydes and Ketones, *Nature*, 1937, **140**, 195.

36 E. W.-G. Diau, C. Kötting and A. H. Zewail, Femtochemistry of Norrish Type-I

Reactions: II. The Anomalous Predissociation Dynamics of Cyclobutanone on the S1 Surface, *ChemPhysChem*, 2001, **2**, 294–309.

37 E. W.-G. Diau, C. Kötting and A. H. Zewail, Femtochemistry of Norrish Type-I Reactions: I. Experimental and Theoretical Studies of Acetone and Related Ketones on the S1 Surface, *ChemPhysChem*, 2001, **2**, 273–293.

38 E. W.-G. Diau, C. Kötting, T. I. Sølling and A. H. Zewail, Femtochemistry of Norrish Type-I Reactions: III. Highly Excited Ketones—Theoretical, *ChemPhysChem*, 2002, **3**, 57–78.

39 S. De Feyter, E. W.-G. Diau and A. H. Zewail, Femtosecond Dynamics of Norrish Type-II Reactions: Nonconcerted Hydrogen-Transfer and Diradical Intermediacy, *Angew. Chemie Int. Ed.*, 2000, **39**, 260–263.

40 D. Shemesh, Z. Lan and R. B. Gerber, Dynamics of Triplet-State Photochemistry of Pentanal: Mechanisms of Norrish I, Norrish II, and H Abstraction Reactions, *J. Phys. Chem. A*, 2013, **117**, 11711–11724.

41 G. M. Roberts and V. G. Stavros, The role of πσ* states in the photochemistry of heteroaromatic biomolecules and their subunits: insights from gas-phase femtosecond spectroscopy, *Chem. Sci.*, 2014, **5**, 1698.

42 N.-C. Yang, E. D. Feit, M. H. Hui, N. J. Turro and J. C. Dalton, Photochemistry of di-tert-butyl ketone and structural effects on the rate and efficiency of intersystem crossing of aliphatic ketones, *J. Am. Chem. Soc.*, 1970, **92**, 6974–6976.

43 M. Fréneau and N. Hoffmann, The Paternò-Büchi reaction—Mechanisms and application to organic synthesis, *J. Photochem. Photobiol. C Photochem. Rev.*, 2017, **33**, 83–108.

44 S. A. Mang, D. K. Henricksen, A. P. Bateman, M. P. S. Andersen, D. R. Blake and S. A.

Nizkorodov, Contribution of Carbonyl Photochemistry to Aging of Atmospheric Secondary Organic Aerosol, *J. Phys. Chem. A*, 2008, **112**, 8337–8344.

45 C. M\oller and M. S. Plesset, Note on an Approximation Treatment for Many-Electron Systems, *Phys. Rev.*, 1934, **46**, 618–622.

46 W. J. Hehre, R. Ditchfield, R. F. Stewart and J. A. Pople, Self-Consistent Molecular Orbital Methods. IV. Use of Gaussian Expansions of Slater-Type Orbitals. Extension to Second-Row Molecules, *J. Chem. Phys.*, 1970, **52**, 2769–2773.

47 C. Peng and H. Bernhard Schlegel, Combining Synchronous Transit and Quasi-Newton Methods to Find Transition States, *Isr. J. Chem.*, 1993, **33**, 449–454.

48 K. Andersson, P. Malmqvist and B. O. Roos, Second-order perturbation theory with a complete active space self-consistent field reference function, *J. Chem. Phys.*, 1992, **96**, 1218–1226.

49 K. Andersson, P. A. Malmqvist, B. O. Roos, A. J. Sadlej and K. Wolinski, Second-order perturbation theory with a CASSCF reference function, *J. Phys. Chem.*, 1990, **94**, 5483–5488.

50 B. O. Roos, P. Linse, P. E. M. Siegbahn and M. R. A. Blomberg, A simple method for the evaluation of the second-order-perturbation energy from external double-excitations with a CASSCF reference wavefunction, *Chem. Phys.*, 1982, **66**, 197–207.

51 M. J. Frisch, G. W. Trucks, H. B. Schlegel, G. E. Scuseria, M. A. Robb, J. R. Cheeseman, G. Scalmani, V. Barone, B. Mennucci, G. A. Petersson, H. Nakatsuji, M. Caricato, X. Li, H. P. Hratchian, A. F. Izmaylov, J. Bloino, G. Zheng, J. L. Sonnenberg, M. Hada, M. Ehara, K. Toyota, R. Fukuda, J. Hasegawa, M. Ishida, T. Nakajima, Y. Honda, O. Kitao, H. Nakai, T. Vreven, J. A. Montgomery Jr., J. E. Peralta, F. Ogliaro, M. Bearpark, J. J.

Heyd, E. Brothers, K. N. Kudin, V. N. Staroverov, R. Kobayashi, J. Normand, K. Raghavachari, A. Rendell, J. C. Burant, S. S. Iyengar, J. Tomasi, M. Cossi, N. Rega, N. J. Millam, M. Klene, J. E. Knox, J. B. Cross, V. Bakken, C. Adamo, J. Jaramillo, R. Gomperts, R. E. Stratmann, O. Yazyev, A. J. Austin, R. Cammi, C. Pomelli, J. W. Ochterski, R. L. Martin, K. Morokuma, V. G. Zakrzewski, G. A. Voth, P. Salvador, J. J. Dannenberg, S. Dapprich, A. D. Daniels, Ö. Farkas, J. B. Foresman, J. V Ortiz, J. Cioslowski and D. J. Fox, *Gaussian 09, Revis. B.01, Gaussian, Inc., Wallingford CT*, 2009.

52 MOLPRO is a package of ab initio programs written by H.-J. Werner, P. J. Knowles, G. Knizia, F. R. Manby, M. Schütz, P. Celani, W. Györffy, D. Kats, T. Korona, R. Lindh, A. Mitrushenkov, G. Rauhut, K. R. Shamasundar, T. B. Adler, R. D. Amos, S. J. Bennie, A. Bernhardsson, A. Berning, D. L. Cooper, M. J. O. Deegan, A. J. Dobbyn, F. Eckert, E. Goll, C. Hampel, A. Hesselmann, G. Hetzer, T. Hrenar, G. Jansen, C. Köppl, S. J. R. Lee, Y. Liu, A. W. Lloyd, Q. Ma, R. A. Mata, A. J. May, S. J. McNicholas, W. Meyer, T. F. {Miller III}, M. E. Mura, A. Nicklaß, D. P. O'Neill, P. Palmieri, D. Peng, K. Pflüger, R. Pitzer, M. Reiher, T. Shiozaki, H. Stoll, A. J. Stone, R. Tarroni, T. Thorsteinsson, M. Wang, M. Welborn, 2018.

53 M. A. Blitz, D. E. Heard and M. J. Pilling, Study of Acetone Photodissociation over the Wavelength Range 248−330 nm: Evidence of a Mechanism Involving Both the Singlet and Triplet Excited States, *J. Phys. Chem. A*, 2006, **110**, 6742–6756.

54 J. M. Anglada, J. González and M. Torrent-Sucarrat, Effects of the substituents on the reactivity of carbonyl oxides. A theoretical study on the reaction of substituted carbonyl oxides with water, *Phys. Chem. Chem. Phys.*, 2011, **13**, 13034–13045.

55 L. F. Pašteka, M. Melicherčík, P. Neogrády and M. Urban, CASPT2 and CCSD(T) calculations of dipole moments and polarizabilities of acetone in excited states, *Mol. Phys.*, 2012, **110**, 2219–2237.

56 K. Alnama, S. Boyé-Péronne, A.-L. Roche and D. Gauyacq, Excited states of C2H4 studied by (3 + 1) and (3 + 2) REMPI spectroscopy: disentangling the lowest Rydberg series from the strong π–π* V ← N transition, *Mol. Phys.*, 2007, **105**, 1743–1756.

57 R. Nádasdi, G. L. Zügner, M. Farkas, S. Dóbé, S. Maeda and K. Morokuma, Inside Cover: Photochemistry of Methyl Ethyl Ketone: Quantum Yields and S1/S0-Diradical Mechanism of Photodissociation (ChemPhysChem 18/2010), *ChemPhysChem*, 2010, **11**, 3774.

58 B. R. Heazlewood, M. J. T. Jordan, S. H. Kable, T. M. Selby, D. L. Osborn, B. C. Shepler, B. J. Braams and J. M. Bowman, Roaming is the dominant mechanism for molecular products in acetaldehyde photodissociation, *Proc. Natl. Acad. Sci.*, 2008, **105**, 12719 LP-12724.

59 S. Maeda, K. Ohno and K. Morokuma, A Theoretical Study on the Photodissociation of Acetone: Insight into the Slow Intersystem Crossing and Exploration of Nonadiabatic Pathways to the Ground State, *J. Phys. Chem. Lett.*, 2010, **1**, 1841–1845.

60 M. R. Nimlos, J. A. Soderquist and G. B. Ellison, Spectroscopy of the acetyl anion CH3CO- and radical CH3CO, *J. Am. Chem. Soc.*, 1989, **111**, 7675–7681.

61 L. A. Baker, B. Marchetti, T. N. V Karsili, V. G. Stavros and M. N. R. Ashfold, Photoprotection: extending lessons learned from studying natural sunscreens to the design of artificial sunscreen constituents, *Chem. Soc. Rev.*, 2017, **46**, 3770–3791.

62 A. A. Beckstead, Y. Zhang, M. S. de Vries and B. Kohler, Life in the light: nucleic acid

photoproperties as a legacy of chemical evolution, *Phys. Chem. Chem. Phys.*, 2016, **18**, 24228–24238.

63 M. Barbatti, Photorelaxation Induced by Water–Chromophore Electron Transfer, *J. Am. Chem. Soc.*, 2014, **136**, 10246–10249.

64 E. B. Abuin, M. V Encina and E. A. Lissi, The photolysis of 3-pentanone, *J. Photochem.*, 1972, **1**, 387–396.

65 A. L. Sobolewski, W. Domcke, C. Dedonder-Lardeux and C. Jouvet, Excited-state hydrogen detachment and hydrogen transfer driven by repulsive 1πσ* states: A new paradigm for nonradiative decay in aromatic biomolecules, *Phys. Chem. Chem. Phys.*, 2002, **4**, 1093–1100.